Featured in Physics

Deceleration and Trapping of SrF Molecules

P. Aggarwal,[1,2,*] Y. Yin,[1,2,*] K. Esajas,[1,2] H. L. Bethlem,[1,3] A. Boeschoten,[1,2] A. Borschevsky,[1,2] S. Hoekstra,[1,2,†] K. Jungmann,[1,2] V. R. Marshall,[1,2] T. B. Meijknecht,[1,2] M. C. Mooij,[2,3] R. G. E. Timmermans,[1,2] A. Touwen,[1,2] W. Ubachs,[3] and L. Willmann[1,2]

(NL-*e*EDM Collaboration)

[1]*Van Swinderen Institute for Particle Physics and Gravity, University of Groningen, Zernikelaan 25, 9747 AA Groningen, The Netherlands*
[2]*Nikhef, National Institute for Subatomic Physics, Science Park 105, 1098 XG Amsterdam, The Netherlands*
[3]*Department of Physics and Astronomy, and LaserLaB, Vrije Universiteit, De Boelelaan 1081, 1081 HV Amsterdam, The Netherlands*

(Received 14 March 2021; accepted 7 September 2021; published 21 October 2021)

We report on the electrostatic trapping of neutral SrF molecules. The molecules are captured from a cryogenic buffer-gas beam source into the moving traps of a 4.5-m-long traveling-wave Stark decelerator. The SrF molecules in $X^2\Sigma^+(v=0, N=1)$ state are brought to rest as the velocity of the moving traps is gradually reduced from 190 m/s to zero. The molecules are held for up to 50 ms in multiple electric traps of the decelerator. The trapped packets have a volume (FWHM) of 1 mm^3 and a velocity spread of 5(1) m/s, which corresponds to a temperature of 60(20) mK. Our result demonstrates a factor 3 increase in the molecular mass that has been Stark decelerated and trapped. Heavy molecules (mass > 100 amu) offer a highly increased sensitivity to probe physics beyond the standard model. This work significantly extends the species of neutral molecules of which slow beams can be created for collision studies, precision measurement, and trapping experiments.

DOI: 10.1103/PhysRevLett.127.173201

Slow beams and trapped samples of heavy diatomic molecules are highly interesting as probes of fundamental physics, specifically for a measurement of the electron's electric dipole moment (*e*EDM) [1–5] and to study parity violation [6]. However, it is challenging to obtain slow beams or even trapped samples of suitable molecules, which are key to achieve increased precision in spectroscopy [7].

Stark deceleration is a successful technique to capture molecules from a supersonic expansion and decelerate them [8]. Beams of ND_3 [9], NH_3 [10], OH [11,12], OD [13], NH [14], CO [15], and CH_3F [16] molecules have been decelerated and trapped using this technique. Some of these decelerated and trapped samples have been used for high-resolution spectroscopy [17], the measurement of collision cross sections [18], and the determination of lifetimes of long-lived electronically and vibrationally excited states [15,19]. Magnetic [20,21] and optical [22] analogs of the decelerator have also been developed. Beams of H_2 and NO molecules in Rydberg states have been decelerated and trapped using a Rydberg Stark decelerator [23,24]. Until now, CH_3F [16] and O_2 [25] are the heaviest molecules to have been trapped following Stark and Zeeman deceleration, respectively. The heavy alkaline-earth monohalide molecules, like SrF and BaF (with a mass of 107 and 156 amu, respectively), are especially interesting for the precision measurements mentioned above [5,6]. However, their energy-level structure and the resulting Stark shifts limited the possible deceleration strength and hereby the final velocities obtained when starting from fast molecular beams [26,27]. This, together with the larger mass, requires a much longer decelerator—but especially at low velocities, switching-type decelerators suffer from instabilities [28] that stand in the way of high-intensity slow beams and trapped samples.

We combine two developments to make the deceleration and trapping of these molecules possible. First, second-generation decelerators, such as the traveling-wave Stark decelerator (TWSD) [27,29–32] and advanced operation of the switching-type decelerators [33,34], allow the stable operation of long decelerators. For this purpose, we have built a 4.5-m-long TWSD. Second, cryogenic buffer-gas molecular beam sources have been developed that, compared to supersonic beams, produce molecules with comparatively higher intensities and a significantly lower velocity of 150–200 m/s [35]. The combination of the intense, slow beam provided by the cryogenic buffer-gas source and the stability of the TWSD has allowed us to decelerate SrF to standstill.

The alkaline-earth monohalides also have been found to be amenable to laser cooling [36]. To date, laser cooling has

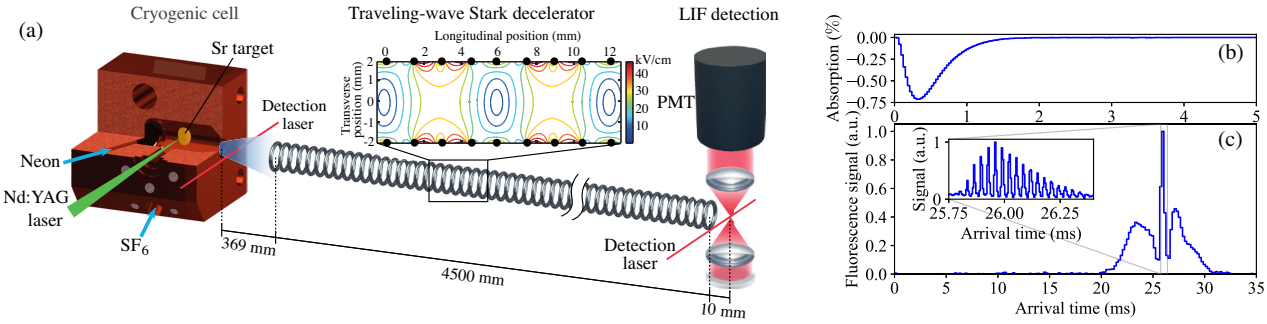

FIG. 1. (a) Experimental setup: The SrF molecules are produced in a cryogenic buffer-gas source. On exiting from the cell, molecules enter the 4.5-m-long TWSD that is mounted 36.9 cm behind the source exit. The molecules travel through the decelerator in the guided or the deceleration mode. They are then detected at a distance of 1 cm from the last ring electrode of the TWSD. (b) The typical absorption signal of the molecular beam measured at a distance of 5 mm from the cell exit. (c) The experimental time-of-flight profile with a bin size of 200 μs, shows the guiding of the molecular beam of SrF with an average velocity of 190 m/s at 5.0 kV. Inset: an enlargement of the guided peak with a bin size of 5 μs, which shows the individual electric field traps filled by the molecules inside the TWSD.

been demonstrated for cryogenic beams of SrF [37,38], CaF [39–42], and YO molecules [43,44]. The heavier molecules [37,45,46] need more repump lasers to close the leaks to other hyperfine, rotational, vibrational, and even electronic levels. Stark deceleration of cryogenic beams therefore expands the range of species that can be decelerated and used for precision measurements [5].

In this Letter, we demonstrate the deceleration and trapping of a SrF molecular beam from a cryogenic source in a 4.5-m-long TWSD. The experimental setup, which is shown in Fig. 1(a), consists mainly of three parts: a cryogenic buffer-gas source, a TWSD, and a laser-induced-fluorescence (LIF) detection section. SrF molecules are produced and cooled in the cryogenic buffer-gas source that uses a two-stage pulse tube cryocooler. The first stage is held at a temperature of 24–26 K and the second stage at a temperature of 4 K. A copper cell whose design is adopted from [47] is attached to the second stage of the cryocooler, and the temperature of the cell is maintained at 17 K via a heater. A 4 mJ, 5 ns laser pulse with a repetition rate of 10 Hz from a Nd:YAG laser at 532 nm ablates a strontium metal target mounted inside the cell. Sulphur hexafluoride (SF_6) gas enters the cell with a flow rate of 0.5 sccm, where it reacts with the ablation products to form SrF. The SrF molecules thermalize with precooled neon, which enters the cell from a different gas line at a flow rate of 8.0 sccm. Molecules are detected at a distance of 5 mm from the cell exit via absorption on the 663 nm transition $A^2\Pi_{1/2}(v' = 0, J' = 1/2) \leftarrow X^2\Sigma^+(v = 0, N = 1)$. The hyperfine structure of the $N = 1$ rotational level in the ground electronic state $X^2\Sigma^+(v = 0, N = 1)$ is covered by adding sidebands to the detection laser. A typical absorption signal of the molecules is shown in Fig. 1(b).

The velocity of SrF molecules in the $X^2\Sigma^+(v = 0, N = 1)$ low-field seeking state with a maximum Stark shift of 0.16 cm^{-1} [31] can be manipulated in the time-dependent inhomogeneous electric field distribution created inside the 4.5-m-long traveling-wave Stark decelerator [27] as shown in the inset of Fig. 1(a). Molecules from the Stark decelerator are detected using LIF. About 1 cm away from the last ring of the decelerator, a diode laser beam with a beam diameter ($1/e^2$) of 0.7 mm and a power of 0.5 mW interacts perpendicularly with the molecular beam, exciting the molecules on the same transition as is used for the absorption detection. The fluorescence emitted from molecules is collected and imaged onto a photomultiplier tube (PMT) by a combination of lenses with a collection solid angle of 0.93 sr and a collection efficiency of 7.5%. The molecular time-of-flight signal is then recorded by making a histogram of the fluorescence photon counts with respect to the arrival time of the molecules, with $t = 0$ ms corresponding to the time at which the Nd:YAG laser ablates the strontium target.

We determined the central velocity of the molecular beam from the cryogenic source by guiding the molecules at different speeds and comparing the strengths of the LIF signals. The guiding velocity that yields the highest intensity in the guiding signal peak was determined to be 190 m/s. This velocity is also employed later as the initial velocity for the deceleration mode of the TWSD.

Figure 1(c) shows a typical time-of-flight LIF signal of the molecules guided at 190 m/s with a 5 kV amplitude sinusoidal voltage applied to the decelerator. A central peak arrives 26 ms after ablation, corresponding to the molecules that are within the longitudinal and transverse phase-space acceptance of the decelerator. These molecules can thus be trapped and guided until the end. The two adjacent wings correspond to the molecules that are outside the longitudinal but inside the transverse acceptance. These molecules are confined transversely while traveling through the decelerator.

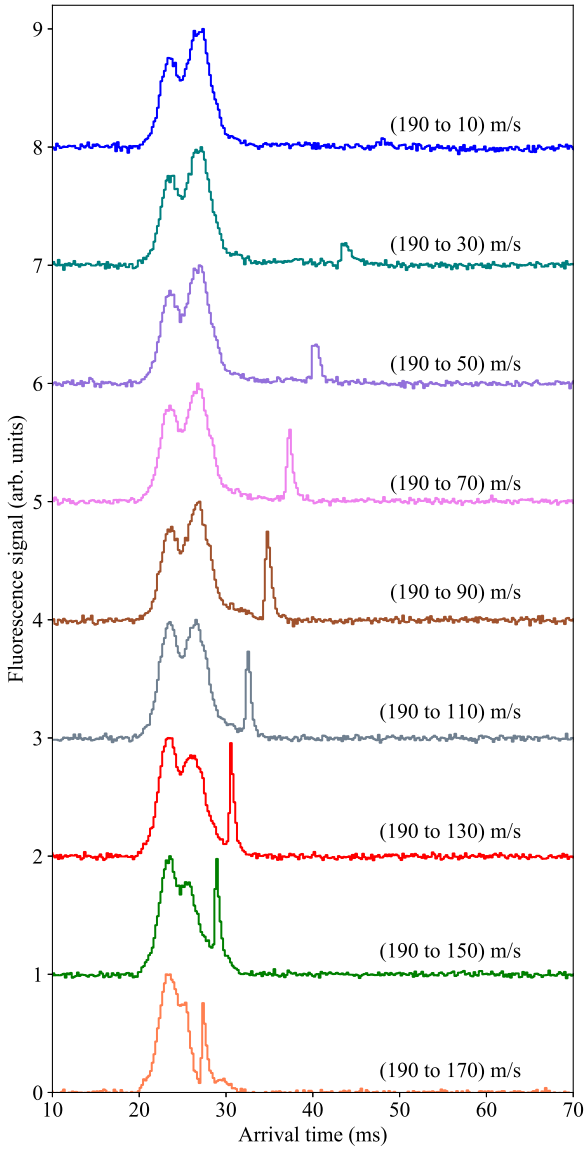

FIG. 2. Time-of-flight LIF signals depicting the deceleration of SrF molecules from 190 m/s to different final velocities until 10 m/s at a voltage amplitude applied to the decelerator of 5 kV with a bin size of 200 μs. A vertical offset has been added to different plots for clarity.

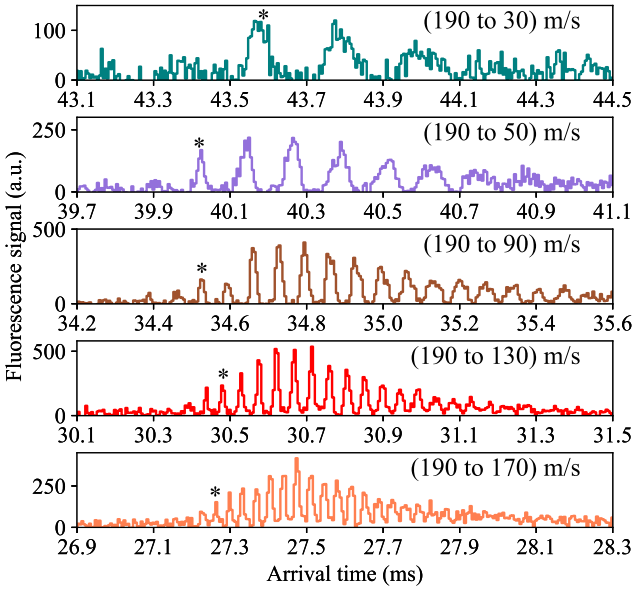

FIG. 3. Enlarged view of the time-of-flight histograms around the arrival time of the decelerated peaks with a bin size of 5 μs, for a few selected final velocities 170, 130, 90, 50, 30 m/s. The peaks labeled (*) correspond to the synchronous molecules, which represent the first packet of molecules that is detected after the electric fields of the decelerator are switched off.

An enlarged view of the guided peak, as shown in the inset of Fig. 1(c), indicates that there are approximately 16 subpeaks within it, which correspond to the molecules trapped in 16 consecutive electric wells inside the decelerator. This is a consequence of the relatively long pulse of molecules from the cryogenic buffer-gas source, in contrast to the guiding of a supersonic molecular beam in the same decelerator [27]. As the periodicity of the electric wells is 6 mm [see Fig. 1(a)], the guided molecular beam packet extends to ~100 mm.

We measured the deceleration of the molecular beam from 190 m/s to a series of final velocities ranging from 170 to 10 m/s. The corresponding time-of-flight signals are shown in Fig. 2 with a bin size of 200 μs, where each plot is averaged over 12 000 ablation shots and a vertical offset has been added to the plots for clarity. There are molecules arriving between 20 and 30 ms, which corresponds to the ones that failed to be trapped longitudinally but were confined transversely (we will refer to them as the nonslowed part of the signal). A fraction of molecules arrive at a later time as we decrease the final velocity of deceleration (which will be referred to as the slowed part). The height of the nonslowed part remains basically the same for all the plots, although the distributions of them are slightly different due to the small variation of the molecular beam properties over our measurement time.

An enlarged view of the slowed part for a number of different final velocities is shown in Fig. 3. The labeled peaks (*) correspond to the packet that contains the synchronous molecules. The electric fields of the decelerator are switched off at the moment that these molecules reach the end of the decelerator. The following peaks correspond to molecules in subsequent traps. Since these packets of molecules have to travel further and thus expand more on their way to the detection volume, this leads to an increased width and reduced intensity in the time-of-flight profile. This explains that for the lower final velocities we detect only the first few of the 16 packets of molecules. In addition, the phase-space acceptance of the decelerator depends on the acceleration; the acceptance for deceleration to 10 m/s is reduced by about a factor of 3 compared to the acceptance at 170 m/s according to the numerical

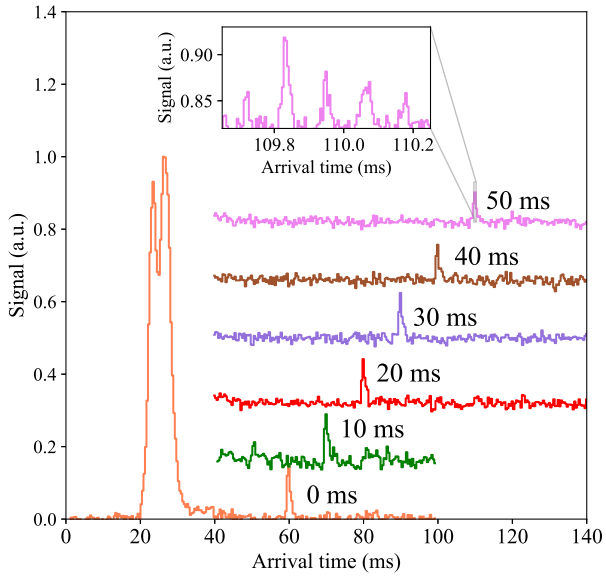

FIG. 4. Time-of-flight histograms with a bin size of 400 μs demonstrating the trapping of SrF molecules for different trapping times Δt. The undecelerated molecules are only shown for the case of $\Delta t = 0$. A vertical offset has been added to the plots for clarity. The inset shows an enlargement of the trapping peak for the case of $\Delta t = 50$ ms.

trajectory simulations [31]. These two factors together account for the observed reduction in the integrated fluorescence signal that can be seen in Fig. 2 for the lower velocities.

By calculating the width difference for adjacent peaks and the difference in their arrival time [48], the full width at half maximum (FWHM) velocity spread of the slowed molecules is 10(2) m/s for molecules decelerated to 170 m/s and 4(1) m/s for molecules decelerated to 50 m/s. The corresponding position spreads of the beams decelerated to 170 and 50 m/s are 2.1(3) and 1.0(2) mm, respectively. The uncertainty of these numbers takes into account the ramp-down time to switch off the electric field on the decelerator (260 μs).

In Fig. 4, we demonstrate the stopping and trapping of the SrF molecules in the lab frame inside the electric traps of the decelerator. SrF molecules are decelerated from 190 to 0 m/s over a length of 4.2 m and held for a trapping time Δt in the inherent electric traps of the decelerator. To detect the trapped molecules, they are accelerated out of the decelerator with the same magnitude of acceleration strength as the deceleration strength, meaning that molecules are accelerated to 52 m/s in the remaining 0.3 m length of the decelerator and detected 1 cm away from the last ring of the decelerator. The acceleration of SrF molecules trapped for different trapping times to the same final velocity also facilitates a good quantitative comparison of the fluorescence signal strength.

The time-of-flight profile for different trapping times (Δt) with a bin size of 400 μs is shown in Fig. 4. Each plot has been averaged over 72 000 shots and a vertical offset is added to subsequent time-of-flight profiles for clarity. The molecules between the arrival time of 20 and 30 ms, similar to the case of deceleration, are those confined in the decelerator only transversely but not longitudinally. A signal peak at 60 ms for the first case demonstrates a case of zero trapping time ($\Delta t = 0$ ms), where the molecules are decelerated to zero and immediately accelerated out. The subsequent plots show the molecules trapped for different trapping times between 10 and 50 ms, resulting in molecules arriving later. For these trapping times, we observe a modest reduction in the signal consistent with the background gas pressure of 7×10^{-7} mbar in the chamber during operation [13]. An enlarged view of the time-of-flight profile around the arrival time of the molecules trapped for 50 ms with a bin size of 5 μs is shown in the inset of Fig. 4. Limited by the spreading of the packets of trapped molecules after the decelerator is switched off, we clearly observe molecules trapped in at least five neighboring electric field traps. The axial and the radial width of a single trap is 1.0(2) mm. The FWHM velocity spread of the trapped molecules is deduced to be about 5(1) m/s, which agrees with the phase-space acceptance of the TWSD [31] and corresponds to a translational temperature of 60(20) mK.

The average number of detected photons per shot from all molecules leaving the decelerator ranges from 10 to 30 in the datasets presented in this Letter. The fraction of photons detected from the decelerated molecules varies between 13% for deceleration to 170 m/s and 1.2% for deceleration to 10 m/s. For the trapping data, 2.8%–1.3% are trapped for 0–50 ms inside the electric traps of the decelerator. To estimate the number of molecules per detected photon, we take into account the velocity-dependent spreading of the packets of molecules after the decelerator is switched off, using the position and velocity spreads determined above. In principle, with sidebands applied to the laser frequency, sufficient laser power, and a suitable magnetic field for remixing dark states, up to ten photons can be scattered on the used transition per SrF molecule [38]. In the current experiments, the number of scattered photons is limited due to the presence of stray electric fields in the detection volume. We estimate that a single molecule scatters on average at most only one photon. Combining these numbers with the fluorescence collection efficiency, we find that the number of molecules in the decelerated beams is of order 1000 for 1% absorption.

We can also estimate the number of decelerated molecules using the density of the molecular beam measurements combined with the calculated phase-space acceptance of the decelerator. From the absorption signal shown in Fig. 1(b), we estimate that $\sim 10^9$ SrF molecules are produced in the $N = 1$ state. Of these molecules, a fraction of 1.5×10^{-6} have a position and velocity that falls

within the acceptance of the decelerator; hence, we expect to decelerate on the order of 1000 molecules per shot, in good agreement with the numbers derived from the LIF data.

With a total of ∼1000 molecules over 16 traps of 1 mm^3 each (at a 10 Hz repetition rate), these numbers are comparable with the first three-dimensional magneto-optical trap (MOT) of SrF molecules using the direct laser cooling technique with a trap density of 600 cm^{-3} [38], and this density has since then been improved by a factor of 40 [49–51]. Potential ways to increase the molecular numbers in our case include implementing a better matching of the cryogenic source to the decelerator with a hexapole guide, by optically pumping the molecules into the state of interest before they enter the decelerator [52], and by increasing the electric field strength of the decelerator to allow deceleration in the $(N = 2)$ state.

In conclusion, we demonstrated the deceleration and trapping of a SrF molecular beam in the state $X^2\Sigma^+(v = 0, N = 1)$ produced in a cryogenic buffer-gas source in a 4.5-m-long TWSD. SrF molecules with an average velocity of 190 m/s are decelerated down to arbitrarily low velocities and are brought to a standstill and trapped for about 50 ms in a series of consecutive electric wells inside the decelerator. Although the SrF molecule is also amenable to laser cooling and trapping, the technique we employ here relies only on its Stark shift. Therefore, this method gives access to molecular species for which laser cooling is not feasible, opening the prospects for controlling more diverse and complex molecular species desirable for many applications in quantum science and technology and new physics searches. Also, lighter molecules with an unfavorable Stark shift over mass ratio [53] can now be decelerated and trapped. The sensitivity to the eEDM, which scales with the third power of the atomic number, furthermore increases linearly with the long interaction time offered by cold and slow beams of heavy molecules. We will therefore apply the principle of the method demonstrated here to BaF, which is a prime candidate to probe physics beyond the standard model of particle physics [5].

The NL-eEDM consortium receives program funding (EEDM-166) from the Netherlands Organisation for Scientific Research (NWO). We acknowledge support from Mike Tarbutt and Stefan Truppe in the design and construction of the cryogenic source. We thank Leo Huisman for technical assistance to the experiment.

*These authors contributed equally to this work.
†s.hoekstra@rug.nl

[1] J. J. Hudson, D. M. Kara, I. J. Smallman, B. E. Sauer, M. R. Tarbutt, and E. A. Hinds, Improved measurement of the shape of the electron, Nature (London) **473**, 493 (2011).
[2] W. B. Cairncross, D. N. Gresh, M. Grau, K. C. Cossel, T. S. Roussy, Y. Ni, Y. Zhou, J. Ye, and E. A. Cornell, Precision Measurement of the Electron's Electric Dipole Moment Using Trapped Molecular Ions, Phys. Rev. Lett. **119**, 153001 (2017).
[3] A. C. Vutha, M. Horbatsch, and E. A. Hessels, Orientation-dependent hyperfine structure of polar molecules in a rare-gas matrix: A scheme for measuring the electron electric dipole moment, Phys. Rev. A **98**, 032513 (2018).
[4] V. Andreev, D. G. Ang, D. DeMille, J. M. Doyle, G. Gabrielse, J. Haefner, N. R. Hutzler, Z. Lasner, C. Meisenhelder, B. R. OLeary, C. D. Panda, A. D. West, E. P. West, and X. Wu (ACME Collaboration), Improved limit on the electric dipole moment of the electron, Nature (London) **562**, 355 (2018).
[5] P. Aggarwal, H. L. Bethlem, A. Borschevsky, M. Denis, K. Esajas, P. A. B. Haase, Y. Hao, S. Hoekstra, K. Jungmann, T. B. Meijknecht, M. C. Mooij, R. G. E. Timmermans, W. Ubachs, L. Willmann, and A. Zapara (NL-eEDM Collaboration), Measuring the electric dipole moment of the electron in BaF, Eur. Phys. J. D **72**, 197 (2018).
[6] E. Altuntaş, J. Ammon, S. B. Cahn, and D. DeMille, Measuring nuclear-spin-dependent parity violation with molecules: Experimental methods and analysis of systematic errors, Phys. Rev. A **97**, 042101 (2018).
[7] M. R. Tarbutt, J. J. Hudson, B. E. Sauer, and E. A. Hinds, Prospects for measuring the electric dipole moment of the electron using electrically trapped polar molecules, Faraday Discuss. **142**, 37 (2009).
[8] S. Y. T. van de Meerakker, H. L. Bethlem, and G. Meijer, Taming molecular beams, Nat. Phys. **4**, 595 (2008).
[9] H. L. Bethlem, G. Berden, M. H. Crompvoets, R. T. Jongma, A. J. A. van Roij, and G. Meijer, Electrostatic trapping of ammonia molecules, Nature (London) **406**, 491 (2000).
[10] H. L. Bethlem, F. M. H. Crompvoets, R. T. Jongma, S. Y. T. van de Meerakker, and G. Meijer, Deceleration and trapping of ammonia using time-varying electric fields, Phys. Rev. A **65**, 053416 (2002).
[11] S. Y. T. van de Meerakker, P. H. M. Smeets, N. Vanhaecke, R. T. Jongma, and G. Meijer, Deceleration and Electrostatic Trapping of OH Radicals, Phys. Rev. Lett. **94**, 023004 (2005).
[12] B. C. Sawyer, B. L. Lev, E. R. Hudson, B. K. Stuhl, M. Lara, J. L. Bohn, and J. Ye, Magnetoelectrostatic Trapping of Ground State OH Molecules, Phys. Rev. Lett. **98**, 253002 (2007).
[13] S. Hoekstra, J. J. Gilijamse, B. Sartakov, N. Vanhaecke, L. Scharfenberg, S. Y. T. van de Meerakker, and G. Meijer, Optical Pumping of Trapped Neutral Molecules by Blackbody Radiation, Phys. Rev. Lett. **98**, 133001 (2007).
[14] S. Hoekstra, M. Metsälä, P. C. Zieger, L. Scharfenberg, J. J. Gilijamse, G. Meijer, and S. Y. T. van de Meerakker, Electrostatic trapping of metastable NH molecules, Phys. Rev. A **76**, 063408 (2007).
[15] J. J. Gilijamse, S. Hoekstra, S. A. Meek, M. Metsl, S. Y. T. van de Meerakker, and G. Meijer, The radiative lifetime of metastable CO ($a^3\Pi$, $\nu = 0$), J. Chem. Phys. **127**, 221102 (2007).

[16] C. Meng, A. P. P. van der Poel, C. Cheng, and H. L. Bethlem, Femtosecond laser detection of Stark-decelerated and trapped methylfluoride molecules, Phys. Rev. A **92**, 023404 (2015).
[17] J. van Veldhoven, J. Kpper, H. L. Bethlem, B. Sartakov, A. J. A. van Roij, and G. Meijer, Decelerated molecular beams for high-resolution spectroscopy, Eur. Phys. J. D **31**, 337 (2004).
[18] J. J. Gilijamse, S. Hoekstra, Y. T. van de Meerakker, G. C. Groenenboom, and G. Meijer, Near-threshold inelastic collisions using molecular beams with a tunable velocity, Science **313**, 1617 (2006).
[19] S. Y. T. van de Meerakker, N. Vanhaecke, M. P. J. van der Loo, G. C. Groenenboom, and G. Meijer, Direct Measurement of the Radiative Lifetime of Vibrationally Excited OH Radicals, Phys. Rev. Lett. **95**, 013003 (2005).
[20] N. Vanhaecke, U. Meier, M. Andrist, B. H. Meier, and F. Merkt, Multistage Zeeman deceleration of hydrogen atoms, Phys. Rev. A **75**, 031402(R) (2007).
[21] E. Narevicius, A. Libson, C. G. Parthey, I. Chavez, J. Narevicius, U. Even, and M. G. Raizen, Stopping supersonic oxygen with a series of pulsed electromagnetic coils: A molecular coilgun, Phys. Rev. A **77**, 051401(R) (2008).
[22] R. Fulton, I. Bishop, M. N. Shneider, and P. F. Barker, Controlling the motion of cold molecules with deep periodic optical potentials, Nat. Phys. **2**, 465 (2006).
[23] S. D. Hogan, C. Seiler, and F. Merkt, Rydberg-State-Enabled Deceleration and Trapping of Cold Molecules, Phys. Rev. Lett. **103**, 123001 (2009).
[24] A. Deller, M. H. Rayment, and S. D. Hogan, Slow Decay Processes of Electrostatically Trapped Rydberg NO Molecules, Phys. Rev. Lett. **125**, 073201 (2020).
[25] N. Akerman, M. Karpov, Y. Segev, N. Bibelnik, J. Narevicius, and E. Narevicius, Trapping of Molecular Oxygen Together with Lithium Atoms, Phys. Rev. Lett. **119**, 073204 (2017).
[26] N. E. Bulleid, R. J. Hendricks, E. A. Hinds, S. A. Meek, G. Meijer, A. Osterwalder, and M. R. Tarbutt, Traveling-wave deceleration of heavy polar molecules in low-field-seeking states, Phys. Rev. A **86**, 021404(R) (2012).
[27] S. C. Mathavan, A. Zapara, Q. Esajas, and S. Hoekstra, Deceleration of a supersonic beam of SrF molecules to 120 ms^{-1}, ChemPhysChem **17**, 3709 (2016).
[28] S. Y. T. van de Meerakker, N. Vanhaecke, H. L. Bethlem, and G. Meijer, Transverse stability in a Stark decelerator, Phys. Rev. A **73**, 023401 (2006).
[29] A. Osterwalder, S. A. Meek, G. Hammer, H. Haak, and G. Meijer, Deceleration of neutral molecules in macroscopic traveling traps, Phys. Rev. A **81**, 051401(R) (2010).
[30] S. A. Meek, M. F. Parsons, G. Heyne, V. Platschkowski, H. Haak, G. Meijer, and A. Osterwalder, A traveling wave decelerator for neutral polar molecules, Rev. Sci. Instrum. **82**, 093108 (2011).
[31] J. E. van den Berg, S. C. Mathavan, C. Meinema, J. Nauta, T. H. Nijbroek, K. Jungmann, H. L. Bethlem, and S. Hoekstra, Traveling-wave deceleration of SrF molecules, J. Mol. Spectrosc. **300**, 22 (2014).
[32] M. Quintero-Pérez, P. Jansen, T. E. Wall, J. E. van den Berg, S. Hoekstra, and H. L. Bethlem, Static Trapping of Polar Molecules in a Traveling Wave Decelerator, Phys. Rev. Lett. **110**, 133003 (2013).
[33] L. Scharfenberg, H. Haak, G. Meijer, and S. Y. T. van de Meerakker, Operation of a Stark decelerator with optimum acceptance, Phys. Rev. A **79**, 023410 (2009).
[34] D. Reens, H. Wu, A. Aeppli, A. McAuliffe, P. Wcisło, T. Langen, and J. Ye, Beyond the limits of conventional Stark deceleration, Phys. Rev. Research **2**, 033095 (2020).
[35] N. R. Hutzler, H. I. Lu, and J. M. Doyle, The buffer gas source: An intense, cold, and slow source for atoms and molecules, Chem. Rev. **112**, 4803 (2012).
[36] N. J. Fitch and M. R. Tarbutt, Chapter Three - Laser-cooled molecules, Adv. At. Mol. Opt. Phys. **70**, 157 (2021).
[37] J. F. Barry, E. S. Shuman, E. B. Norrgard, and D. DeMille, Laser Radiation Pressure Slowing of a Molecular Beam, Phys. Rev. Lett. **108**, 103002 (2012).
[38] J. F. Barry, D. J. McCarron, E. B. Norrgard, M. H. Steinecker, and D. DeMille, Magneto-optical trapping of a diatomic molecule, Nature (London) **512**, 286 (2014).
[39] V. Zhelyazkova, A. Cournol, T. E. Wall, A. Matsushima, J. J. Hudson, E. A. Hinds, M. R. Tarbutt, and B. E. Sauer, Laser cooling and slowing of CaF molecules, Phys. Rev. A **89**, 053416 (2014).
[40] B. Hemmerling, E. Chae, A. Ravi, L. Anderegg, G. K. Drayna, N. R. Hutzler, A. L. Collopy, J. Ye, W. Ketterle, and J. M. Doyle, Laser slowing of CaF molecules to near the capture velocity of a molecular MOT, J. Phys. B **49**, 174001 (2016).
[41] L. Anderegg, B. L. Augenbraun, E. Chae, B. Hemmerling, N. R. Hutzler, A. Ravi, A. Collopy, J. Ye, W. Ketterle, and J. M. Doyle, Radio Frequency Magneto-Optical Trapping of CaF with High Density, Phys. Rev. Lett. **119**, 103201 (2017).
[42] H. J. Williams, S. Truppe, M. Hambach, L. Caldwell, N. J. Fitch, E. A. Hinds, B. E. Sauer, and M. R. Tarbutt, Characteristics of a magneto-optical trap of molecules, New J. Phys. **19**, 113035 (2017).
[43] M. T. Hummon, M. Yeo, B. K. Stuhl, A. L. Collopy, Y. Xia, and J. Ye, 2D Magneto-Optical Trapping of Diatomic Molecules, Phys. Rev. Lett. **110**, 143001 (2013).
[44] A. L. Collopy, S. Ding, Y. Wu, I. A. Finneran, L. Anderegg, B. L. Augenbraun, J. M. Doyle, and J. Ye, 3D Magneto-Optical Trap of Yttrium Monoxide, Phys. Rev. Lett. **121**, 213201 (2018).
[45] Y. Hao, L. F. Pašteka, L. Visscher, P. Aggarwal, H. L. Bethlem, A. Boeschoten, A. Borschevsky, M. Denis, K. Esajas, S. Hoekstra, K. Jungmann, V. R. Marshall, T. B. Meijknecht, M. C. Mooij, R. G. E. Timmermans, A. Touwen, W. Ubachs, L. Willmann, Y. Yin, and A. Zapara, High accuracy theoretical investigations of CaF, SrF, and BaF and implications for laser-cooling, J. Chem. Phys. **151**, 034302 (2019).
[46] T. A. Isaev, S. Hoekstra, and R. Berger, Laser-cooled RaF as a promising candidate to measure molecular parity violation, Phys. Rev. A **82**, 052521 (2010).
[47] S. Truppe, M. Hambach, S. M. Skoff, N. E. Bulleid, J. S. Bumby, R. J. Hendricks, E. A. Hinds, B. E. Sauer, and M. R. Tarbutt, A buffer gas beam source for short, intense and slow molecular pulses, J. Mod. Opt. **65**, 648 (2018).

[48] J. van Veldhoven, H. L. Bethlem, M. Schnell, and G. Meijer, Versatile electrostatic trap, Phys. Rev. A **73**, 063408 (2006).

[49] D. J. McCarron, E. B. Norrgard, M. H. Steinecker, and D. DeMille, Improved magnetooptical trapping of a diatomic molecule, New J. Phys. **17**, 035014 (2015).

[50] E. B. Norrgard, D. J. McCarron, M. H. Steinecker, M. R. Tarbutt, and D. DeMille, Submillikelvin Dipolar Molecules in a Radio-Frequency Magneto-Optical Trap, Phys. Rev. Lett. **116**, 063004 (2016).

[51] M. H. Steinecker, D. J. McCarron, Y. Zhu, and D. DeMille, Improved radio-frequency magneto-optical trap of SrF molecules, ChemPhysChem **17**, 3664 (2016).

[52] C. J. Ho, J. A. Devlin, I. M. Rabey, P. Yzombard, S. C. Wright, N. J. Fitch, E. A. Hinds, M. R. Tarbutt, and B. E. Sauer, New techniques for a measurement of the electron's electric dipole moment, New J. Phys. **22**, 053031 (2020).

[53] M. Motsch, L. D. van Buuren, C. Sommer, M. Zeppenfeld, G. Rempe, and P. W. H. Pinkse, Cold guided beams of water isotopologs, Phys. Rev. A **79**, 013405 (2009).